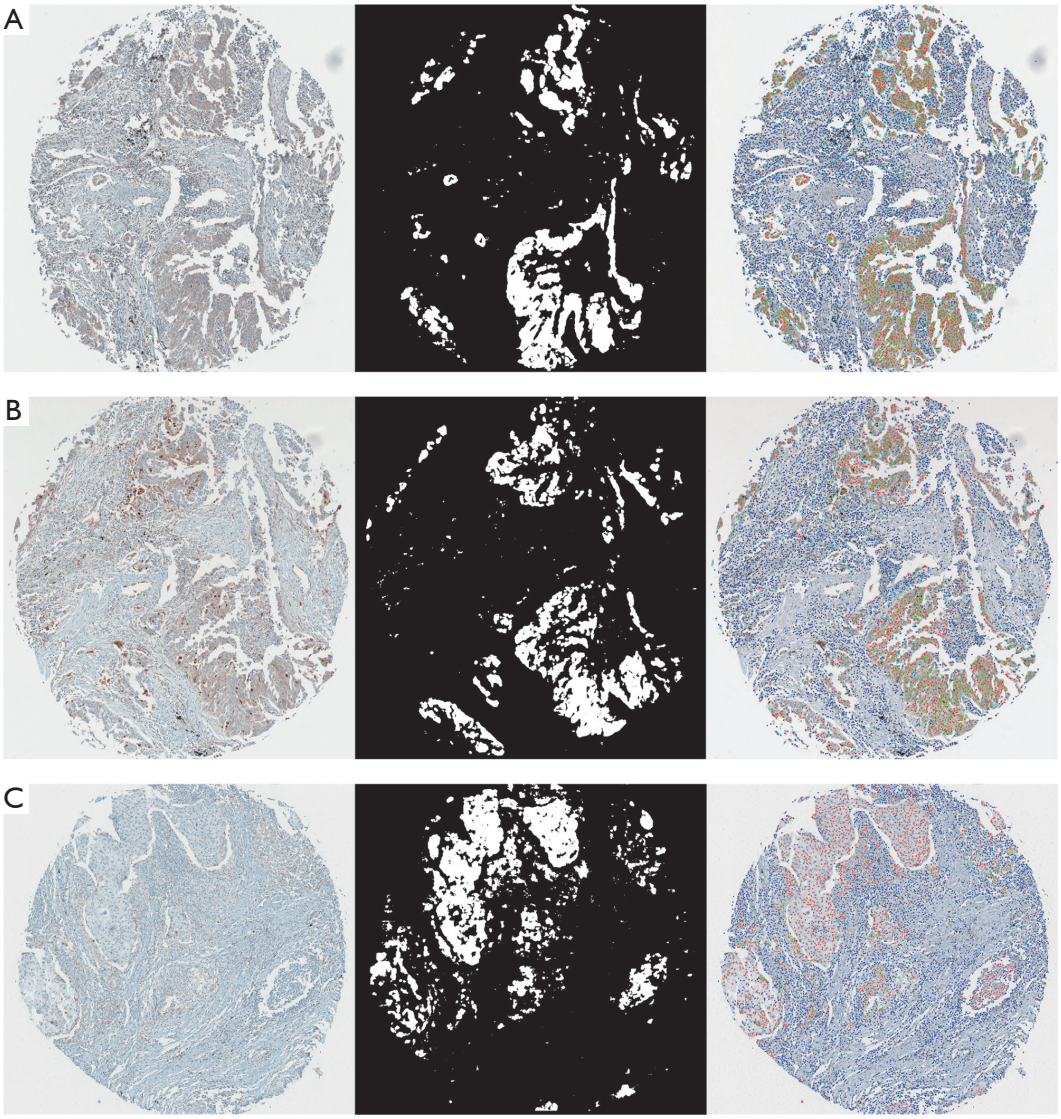

Figure S1 The representative images of segmentation and spatial analysis of the internal cohort. The original IHC image (left), tumor region segmentation mask (middle), and the four classifications of cells (right) of KIR2D (A), galectin-9 (B), and TIM-3 (C). IHC, immunohistochemistry; KIR2D, killer cell immunoglobulin-like receptor-2D; TIM-3, T cell immunoglobulin-3. (A-C) were in ×6.2 magnification.

http://dx.doi.org/10.21037/tlcr-21-96

Table S1 Clinical characteristics of patients in the internal cohort and the external cohort

	Internal cohort (n=121)	External cohort (n=30)	P
Sex			0.476
Male	96	22	
Female	25	8	
Age, Years			0.758
<70	92	22	
≥70	29	8	
Surgery procedures			0.004
Lobectomy	62	26	
Non-lobectomy	59	4	
TNM-stage			<0.0001
I	121	13	
II	0	10	
III	0	7	
Smoking status			<0.0001
No	4	21	
Yes	117	9	
Histology			0.0003
Adenocarcinoma	38	20	
Non-adenocarcinoma	85	10	

http://dx.doi.org/10.21037/tlcr-21-96

Table S2 Univariate cox regression of OS and RFS

Classification	Factor	OS				Factor	RFS			
		No	HR	95% CI	P value		No	HR	95% CI	P value
Distance between positive TILs (one positive TIL to another positive TIL)	TIM-3					TIM-3				
	Near (≤84.76 px)	49	1.000			Near (≤231.05 px)	47	1.000		
	Far (>84.76 px)	33	1.465	(0.869-2.469)	0.152	Far (>231.05 px)	23	0.804	(0.349-1.641)	0.549
	PD-L1					PD-L1				
	Near (≤125.34 px)	71	1.000			Near (≤21.70 px)	17	1.000		
	Far (>125.34 px)	17	1.511	(0.837-2.730)	0.171	Far (>21.70 px)	71	1.422	(0.802-2.522)	0.229
	PD-1					PD-1				
	Near (≤24.00 px)	27	1.000			Near (≤24.00 px)	27	1.000		
	Far (>24.00 px)	74	1.975	(1.078-3.618)	0.028	Far (>24.00 px)	74	1.584	(0.880-2.851)	0.125
	OX40L					OX40L				
	Near (≤48.14 px)	92	1.000			Near (≤61.55 px)	98	1.000		
	Far (>48.14 px)	23	1.788	(1.076-2.989)	0.025	Far (>61.55 px)	17	1.801	(1.032-3.144)	0.038
	OX40					OX40				
	Near (≤98.33 px)	92	1.000			Near (≤87.19 px)	89	1.000		
	Far (>98.33 px)	26	1.752	(1.078-2.846)	0.024	Far (>87.19 px)	29	1.502	(0.938-2.404)	0.090
	MHC-II					MHC-II				
	Near (≤20.87 px)	98	1.000			Near (≤14.94 px)	57	1.000		
	Far (>20.87 px)	14	1.622	(0.874-3.008)	0.125	Far (>14.94 px)	55	0.790	(0.505-1.234)	0.300
	LAG-3					LAG-3				
	Near (≤22.11 px)	29	1.000			Near (≤21.56 px)	28	1.000		
	Far (>22.11 px)	70	1.503	(0.855-2.640)	0.157	Far (>21.56 px)	71	1.444	(0.824-2.531)	0.199
	galectin9					galectin9				
	Near (≤18.27 px)	44	1.000			Near (≤15.55 px)	22	1.000		
	Far (>18.27 px)	61	1.365	(0.833-2.237)	0.216	Far (>15.55 px)	83	0.609	(0.355-1.043)	0.071
	KIR-2D					KIR-2D				
	Near (≤29.34 px)	69	1.000			Near (≤14.71 px)	16	1.000		
	Far (>29.34 px)	40	1.467	(0.918-2.343)	0.109	Far (>14.71 px)	93	0.696	(0.374-1.294)	0.252
	KIR-3D					KIR-3D				
	Near (≤13.44 px)	13	1.000			Near (≤12.91 px)	8	1.000		
	Far (>13.44 px)	96	0.416	(0.217-0.799)	0.008	Far (>12.91 px)	101	0.707	(0.306-1.633)	0.416
Distance between positive TCs (one positive TC to another positive TC)	TIM-3					TIM-3				
	Near (≤546.86 px)	59	1.000			Near (≤261.57 px)	47	1.000		
	Far (>546.86 px)	11	2.039	(1.032-4.030)	0.040	Far (>261.57 px)	23	0.649	(0.349-1.208)	0.173
	PD-L1					PD-L1				
	Near (≤17.97 px)	12	1.000			Near (≤115.32 px)	40	1.000		
	Far (>17.97 px)	65	1.758	(0.751-4.115)	0.193	Far (>115.32 px)	37	1.637	(0.955-2.807)	0.073
	OX40L					OX40L				
	Near (≤141.50 px)	82	1.000			Near (≤141.50 px)	82	1.000		
	Far (>141.50 px)	27	1.674	(1.010-2.744)	0.046	Far (>141.50 px)	27	1.479	(0.898-2.437)	0.125
	OX40					OX40				
	Near (≤236.36 px)	91	1.000			Near (≤31.22 px)	23	1.000		
	Far (>236.36 px)	20	0.647	(0.340-1.229)	0.184	Far (>31.22 px)	88	1.515	(0.817-2.811)	0.187
	MHC-II					MHC-II				
	Near (≤24.37 px)	13	1.000			Near (≤25.36 px)	15	1.000		
	Far (>24.37 px)	96	2.394	(0.965-5.841)	0.060	Far (>25.36 px)	94	1.846	(0.946-4.028)	0.123
	galectin9					galectin9				
	Near (≤85.97 px)	65	1.000			Near (≤119.40 px)	75	1.000		
	Far (>85.97 px)	35	1.820	(1.105-2.999)	0.019	Far (>119.40 px)	25	1.719	(1.002-2.949)	0.049
	KIR-2D					KIR-2D				
	Near (≤24.22 px)	68	1.000			Near (≤26.35 px)	70	1.000		
	Far (>24.22 px)	39	1.849	(1.151-2.969)	0.011	Far (>26.35 px)	37	1.490	(0.926-2.397)	0.100
	KIR-3D					KIR-3D				
	Near (≤16.45 px)	35	1.000			Near (≤16.45 px)	35	1.000		
	Far (>16.45 px)	71	0.838	(0.511-1.373)	0.483	Far (>16.45 px)	71	0.855	(0.525-1.392)	0.529
Distance between positive TCs and positive TILs (one positive TC to one positive TIL)	TIM-3					TIM-3				
	Near (≤190.54 px)	57	1.000			Near (≤52.41 px)	17	1.000		
	Far (>190.54 px)	18	1.664	(0.921-3.008)	0.092	Far (>52.41 px)	58	1.664	(0.921-3.008)	0.092
	PD-L1					PD-L1				
	Near (≤23.99 px)	8	1.000			Near (≤33.58 px)	13	1.000		
	Far (>23.99 px)	71	0.489	(0.220-1.088)	0.080	Far (>33.58 px)	66	0.605	(0.311-1.175)	0.138
	OX40L					OX40L				
	Near (≤40.02 px)	50	1.000			Near (≤40.02 px)	50	1.000		
	Far (>40.02 px)	62	0.570	(0.361-0.902)	0.016	Far (>40.02 px)	62	0.576	(0.366-0.906)	0.017
	OX40					OX40				
	Near (≤94.06 px)	70	1.000			Near (≤94.06 px)	70	1.000		
	Far (>94.06 px)	43	0.681	(0.425-1.093)	0.111	Far (>94.06 px)	43	0.713	(0.448-1.136)	0.155
	MHC-II					MHC-II				
	Near (≤18.68 px)	13	1.000			Near (≤123.11 px)	97	1.000		
	Far (>18.68 px)	97	0.374	(0.200-0.699)	0.002	Far (>123.11 px)	13	1.293	(0.664-2.518)	0.449
	galectin9					galectin9				
	Near (≤83.69 px)	85	1.000			Near (≤24.18 px)	16	1.000		
	Far (>83.69 px)	18	1.384	(0.765-2.502)	0.283	Far (>24.18 px)	87	0.580	(0.316-1.063)	0.078
	KIR-2D					KIR-2D				
	Near (≤66.66 px)	72	1.000			Near (≤44.10 px)	54	1.000		
	Far (>66.66 px)	36	1.452	(0.901-2.341)	0.126	Far (>44.10 px)	54	0.690	(0.434-1.098)	0.117
	KIR-3D					KIR-3D				
	Near (≤20.28 px)	35	1.000			Near (≤20.28 px)	35	1.000		
	Far (>20.28 px)	73	2.337	(1.366-3.977)	0.002	Far (>20.28 px)	73	2.444	(1.379-4.330)	0.002
Distance between all TCs and TILs (one TC to one TIL)	Near (≤44.41 px)	83	1.000			Near (≤60.73 px)	100	1.000		
	Far (>44.41 px)	38	1.672	(1.069-2.614)	0.024	Far (>60.73 px)	21	1.471	(0.868-2.492)	0.152
Distance between TCs and positive TILs (one TC to one positive TIL)	TIM-3					TIM-3				
	Near (≤487.68 px)	71	1.000			Near (≤203.11 px)	40	1.000		
	Far (>487.68 px)	12	1.850	(0.949-3.609)	0.071	Far (>203.11 px)	43	1.317	(0.786-2.207)	0.296
	PD-L1					PD-L1				
	Near (≤104.22 px)	24	1.000			Near (≤46.37 px)	10	1.000		
	Far (>104.22 px)	68	1.535	(0.833-2.829)	0.170	Far (>46.37 px)	68	0.534	(0.264-1.083)	0.082
	PD-1					PD-1				
	Near (≤76.70 px)	29	1.000			Near (≤190.90 px)	69	1.000		
	Far (>76.70 px)	72	1.738	(0.979-3.084)	0.059	Far (>190.90 px)	32	1.461	(0.904-2.362)	0.121
	OX40L					OX40L				
	Near (≤173.56 px)	96	1.000			Near (≤38.24 px)	39	1.000		
	Far (>173.56 px)	20	1.731	(1.025-2.922)	0.040	Far (>38.24 px)	77	0.709	(0.445-1.129)	0.147
	OX40					OX40				
	Near (≤445.89 px)	104	1.000			Near (≤39.20 px)	21	1.000		
	Far (>445.89 px)	14	1.777	(0.991-3.187)	0.054	Far (>39.20 px)	97	0.653	(0.372-1.146)	0.138
	MHC-II					MHC-II				
	Near (≤44.03 px)	49	1.000			Near (≤135.56 px)	96	1.000		
	Far (>44.03 px)	63	1.415	(0.915-2.299)	0.113	Far (>135.56 px)	16	1.761	(0.984-3.150)	0.057
	LAG-3					LAG-3				
	Near (≤184.44 px)	66	1.000			Near (≤184.44 px)	66	1.000		
	Far (>184.44 px)	33	1.593	(0.977-2.597)	0.062	Far (>184.44 px)	33	1.441	(0.885-2.346)	0.142
	galectin9					galectin9				
	Near (≤137.38 px)	87	1.000			Near (≤34.01 px)	23	1.000		
	Far (>137.78 px)	18	1.601	(0.900-2.850)	0.109	Far (>34.01 px)	82	0.689	(0.402-1.181)	0.175
	KIR-2D					KIR-2D				
	Near (≤223.71 px)	93	1.000			Near (≤38.45 px)	40	1.000		
	Far (>223.71 px)	16	1.833	(1.031-3.258)	0.039	Far (>38.45 px)	69	0.694	(0.434-1.110)	0.127
	KIR-3D					KIR-3D				
	Near (≤21.19 px)	35	1.000			Near (≤21.19 px)	35	1.000		
	Far (>21.19 px)	74	2.235	(1.208-3.901)	0.005	Far (>21.19 px)	74	2.017	(1.181-3.443)	0.010
Percentage of positive TILs	TIM-3					TIM-3				
	Low (=0)	4	1.000			Low (≤19%)	69	1.000		
	High (>0)	83	0.513	(0.185-1.422)	0.200	High (>19%)	18	1.523	(0.850-2.731)	0.158
	PD-L1					PD-L1				
	Low (≤21%)	68	1.000			Low (≤2%)	34	1.000		
	High (>21%)	26	0.748	(0.420-1.333)	0.325	High (>2%)	60	1.364	(0.817-2.278)	0.235
	PD-1					PD-1				
	Low (≤3%)	20	1.000			Low (≤51%)	91	1.000		
	High (>3%)	83	0.802	(0.459-1.399)	0.437	High (>51%)	12	1.656	(0.847-3.237)	0.141
	OX40L					OX40L				
	Low (≤68%)	93	1.000			Low (≤48%)	39	1.000		
	High (>68%)	23	1.489	(0.878-2.527)	0.140	High (>43%)	77	1.443	(0.927-2.246)	0.104
	OX40					OX40				
	Low (≤44%)	84	1.000			Low (≤52%)	95	1.000		
	High (>44%)	24	1.739	(1.087-2.781)	0.026	High (>52%)	23	2.015	(1.201-3.383)	0.008
	MHC-II					MHC-II				
	Low (≤92%)	87	1.000			Low (≤92%)	87	1.000		
	High (>92%)	25	1.476	(0.899-2.424)	0.124	High (>92%)	25	1.547	(0.9236-2.556)	0.089
	LAG-3					LAG-3				
	Low (≤55%)	77	1.000			Low (≤55%)	77	1.000		
	High (>55%)	25	0.577	(0.315-1.057)	0.075	High (>55%)	25	0.656	(0.365-1.179)	0.158
	galectin9					galectin9				
	Low (≤23%)	22	1.000			Low (≤20%)	20	1.000		
	High (>23%)	83	1.964	(1.002-3.850)	0.049	High (>20%)	85	2.053	(1.016-4.149)	0.045
	KIR-2D					KIR-2D				
	Low (≤37%)	46	1.000			Low (≤85%)	95	1.000		
	High (>37%)	83	0.593	(0.373-0.944)	0.028	High (>85%)	14	1.699	(0.892-3.234)	0.107
	KIR-3D					KIR-3D				
	Low (≤99%)	84	1.000			Low (≤85%)	26	1.000		
	High (>99%)	25	0.327	(0.128-0.836)	0.020	High (>85%)	83	0.327	(0.128-0.833)	0.019
Percentage of positive TCs	TIM-3					TIM-3				
	Low (=0)	12	1.000			Low (=0)	12	1.000		
	High (>0)	75	0.721	(0.365-1.425)	0.347	High (>0)	75	0.969	(0.477-1.968)	0.931
	PD-L1					PD-L1				
	Low (≤33%)	79	1.000			Low (≤1%)	44	1.000		
	High (>33%)	15	0.619	(0.295-1.300)	0.205	High (>1%)	50	1.462	(0.898-2.383)	0.127
	OX40L					OX40L				
	Low (≤5%)	34	1.000			Low (≤24%)	57	1.000		
	High (>5%)	82	0.689	(0.432-1.100)	0.118	High (>24%)	59	1.268	(0.815-1.973)	0.293
	OX40					OX40				
	Low (≤1%)	8	1.000			Low (≤54%)	106	1.000		
	High (>1%)	110	0.610	(0.293-1.270)	0.186	High (>54%)	12	1.355	(0.677-2.711)	0.390
	MHC-II					MHC-II				
	Low (≤93%)	99	1.000			Low (≤8%)	47	1.000		
	High (>93%)	13	0.425	(0.185-0.979)	0.044	High (>8%)	65	0.828	(0.529-1.296)	0.409
	galectin9					galectin9				
	Low (≤41%)	85	1.000			Low (≤41%)	85	1.000		
	High (>41%)	20	0.450	(0.223-0.909)	0.026	High (>41%)	20	0.606	(0.318-1.157)	0.129
	KIR-2D					KIR-2D				
	Low (≤34%)	7	1.000			Low (≤69%)	84	1.000		
	High (>34%)	102	0.594	(0.257-1.373)	0.223	High (>69%)	25	0.694	(0.387-1.244)	0.220
	KIR-3D					KIR-3D				
	Low (≤99%)	95	1.000			Low (≤67%)	20	1.000		
	High (>99%)	14	0.561	(0.325-0.968)	0.038	High (>67%)	89	0.621	(0.356-1.082)	0.093
Clinical factors	Age					Age				
	≤70	92	1.000			≤70	92	1.000		
	>70	29	0.781	(0.463-1.317)	0.354	>70	29	0.781	(0.463-1.317)	0.354
	Sex					Sex				
	Female	25	1.000			Female	25	1.000		
	Male	96	1.798	(0.973-3.322)	0.061	Male	96	1.360	(0.776-2.382)	0.283
	Smoke					Smoke				
	No	4	1.000			No	4	1.000		
	Yes	117	0.672	(0.212-2.131)	0.500	Yes	117	0.593	(0.187-1.881)	0.375
	Surgery type					Surgery type				
	Wedge	2	1.000			Wedge	2	1.000		
	Segmentectomy	3	9534.267	(0-3.547E+56)		Segmentectomy	3	9252.710	(0-3.749E+55)	
	Lobectomy	62	7210.961	(0-2.663E+56)		Lobectomy	62	7346.015	(0-2.954E+55)	
	Bilobectomy	7	6049.498	(0-2.242E+56)		Bilobectomy	7	6128.606	(0-2.473E+55)	
	Pneumonectomy	41	14177.646	(0-5.236E+56)		Pneumonectomy	41	13559.173	(0-5.452E+55)	
	Sleeve lobectomy	6	10961.091	(0-4.059E+56)	0.020	Sleeve lobectomy	6	10791.431	(0-4.351E+55)	0.066
	Pathology					Pathology				
	Adenocarcinoma	38	1.000			Adenocarcinoma	38	1.000		
	Non-adenocarcinoma	85	1.678	(1.004-2.806)	0.048	Non-adenocarcinoma	85	1.591	(0.968-2.613)	0.067
	T-stage					T-stage				
	1	85	1.000			1	85	1.000		
	2	36	2.011	(1.260-3.210)	0.003	2	36	1.694	(1.061-2.704)	0.027
	N-stage					N-stage				
	0	63	1.000			0	63	1.000		
	1	58	2.479	(1.586-3.873)	<0.0001	1	58	2.510	(1.611-3.910)	<0.0001
	M-stage					M-stage				
	0	114	1.000			0	114	1.000		
	1	7	4.019	(1.803-8.961)	0.001	1	7	3.855	(1.734-8.574)	0.001
	Stage					Stage				
	1A	80	1.000			1A	80	1.000		
	1B	41	5.188	(3.242-8.301)	<0.0001	1B	41	4.092	(2.574-6.504)	<0.0001

Abbreviations: No, number of each class; HR, hazard ratio; OS, overall survival; RFS, relapse-free survival; TC, tumor cell; TIL, tumor-infiltrating lymphocyte; KIR2D, killer cell immunoglobulin-like receptor-2D; KIR-3D, killer cell immunoglobulin-like receptor-3D; TIM-3, T cell immunoglobulin-3; LAG-3, lymphocyte activation gene-3; PD-1, programmed cell death receptor-1; PD-L1, programmed cell death ligand-1; MHC-II, major histocompatibility complex class II; OX40L, OX40-ligand. *All cut-off points were determined by the X-Tile software.

http://dx.doi.org/10.21037/tlcr-21-96

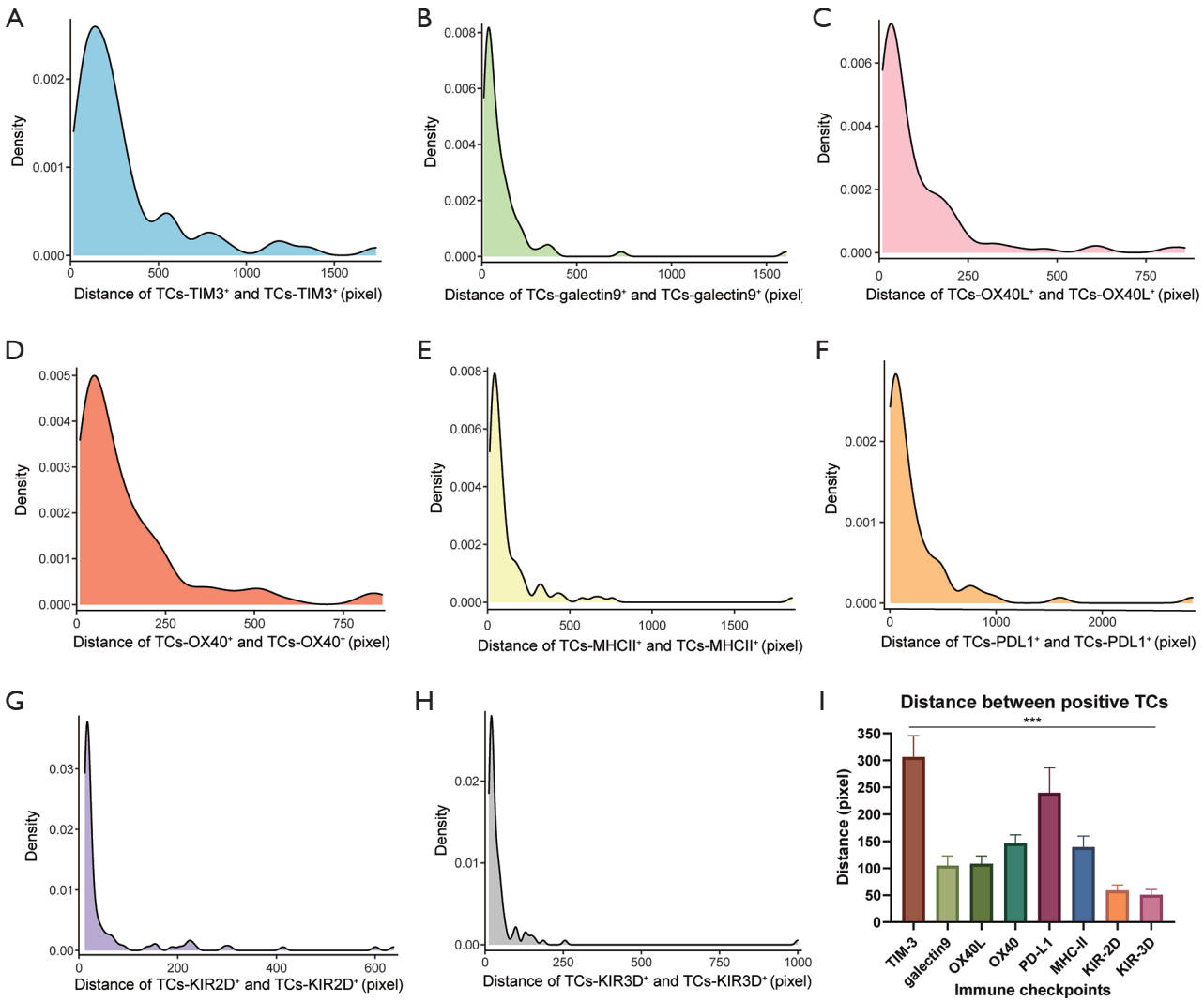

Figure S2 The distribution of the distance between positive TCs (one positive TC to another positive TC). Density curves of the distance of TC $_{TIM3+}$ (A), TC $_{galectin\text{-}9+}$ (B), TC $_{OX40L+}$ (C), TC $_{OX40+}$ (D), TC $_{MHC\text{-}II+}$ (E), TC $_{PD\text{-}L1+}$ (F), TC-$_{KIR2D+}$ (G), TC$_{KIR3D+}$ (H). (I) The column chart of mean distances of positive TCs; P<0.001. **Figures S1A* to *1H* were drawn by the "ggplot" package of R software. TC, tumor cell; KIR2D, killer cell immunoglobulin-like receptor-2D; KIR-3D, killer cell immunoglobulin-like receptor-3D; TIM-3, T cell immunoglobulin-3; LAG-3, lymphocyte activation gene-3; PD-L1, programmed cell death ligand-1; MHC-II, major histocompatibility complex class II; OX40L, OX40-ligand.

http://dx.doi.org/10.21037/tlcr-21-96

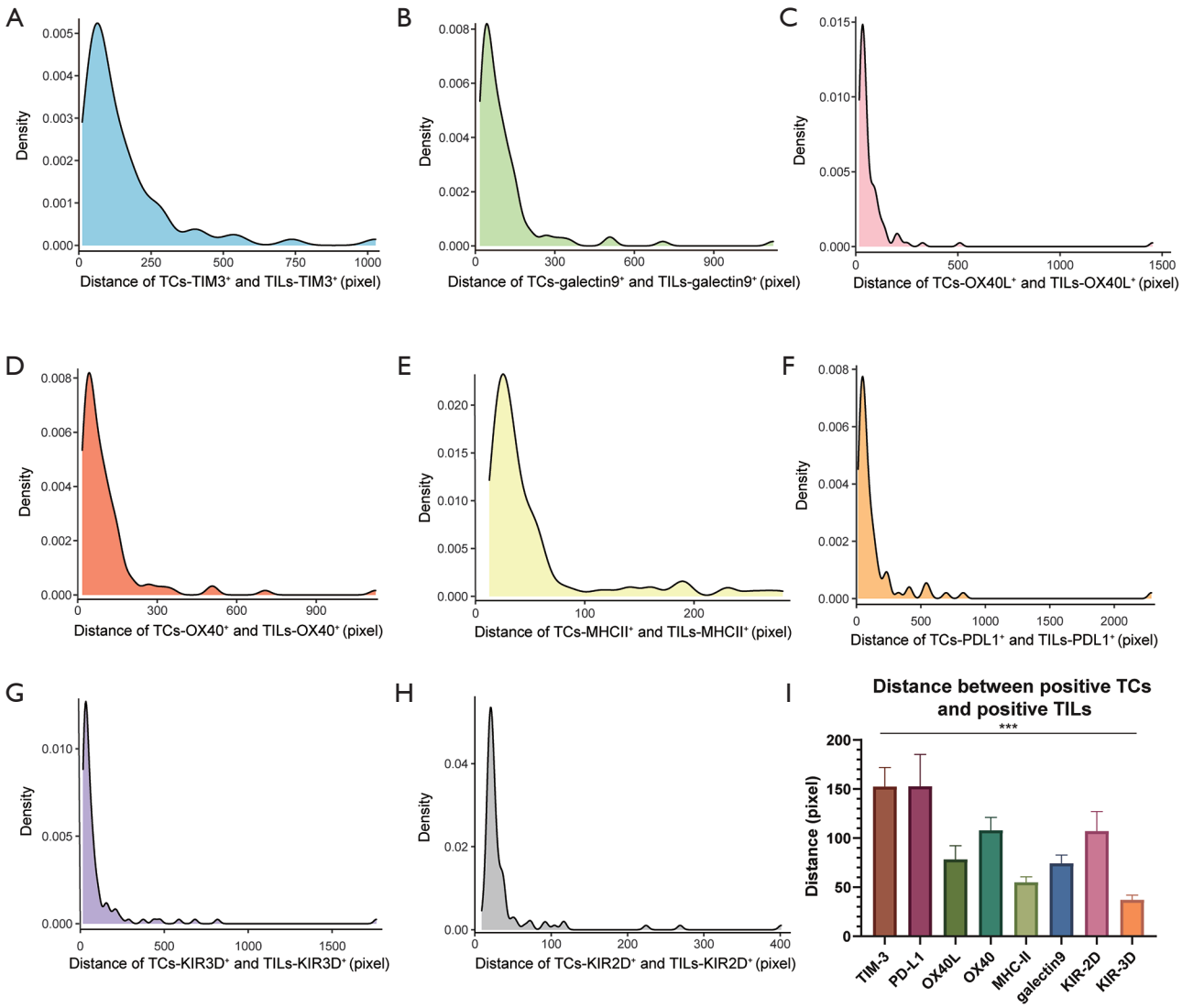

Figure S3 The distribution of the distance between positive TCs and positive TILs (one positive TC to another positive TIL). Density curves of the distance of TC $_{TIM3+}$ and TIL $_{TIM3+}$ (A), TC $_{galectin-9+}$ and TIL $_{galectin-9+}$ (B), TC $_{OX40L+}$ and TIL $_{OX40L+}$ (C), TC $_{OX40+}$ and TIL $_{OX40+}$ (D), TC $_{MHC-II+}$ and TIL $_{MHC-II+}$ (E), TC $_{PD-L1+}$ and TIL $_{PD-L1+}$ (F), TC-$_{KIR2D+}$ and TIL-$_{KIR2D+}$ (G), TC$_{KIR3D+}$ and TIL$_{KIR3D+}$ (H). (I) The column chart of mean distances of positive TCs and positive TILs; P<0.001. **Figures S2A* to *1H* were drawn by the "ggplot" package of R software. TC, tumor cell; TIL, tumor-infiltrating lymphocyte; KIR2D, killer cell immunoglobulin-like receptor-2D; KIR-3D, killer cell immunoglobulin-like receptor-3D; TIM-3, T cell immunoglobulin-3; LAG-3, lymphocyte activation gene-3; PD-L1, programmed cell death ligand-1; MHC-II, major histocompatibility complex class II; OX40L, OX40-ligand.

http://dx.doi.org/10.21037/tlcr-21-96

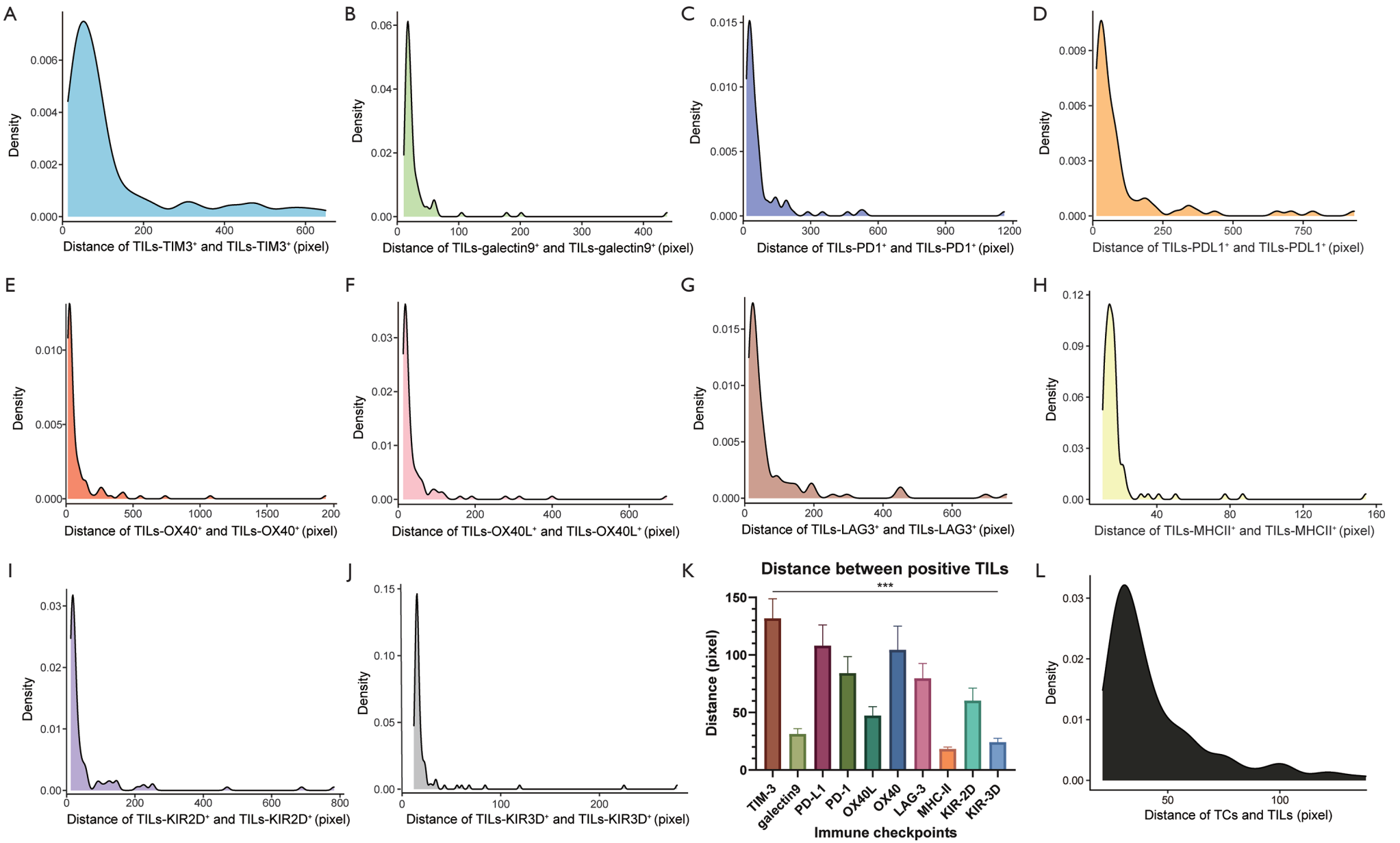

Figure S4 The distribution of the distance between positive TILs (one positive TIL to another positive TIL), and the distance between TCs and TILs (one TC to one TIL). Density curves of the distance of TIL $_{TIM3+}$ and TIL $_{TIM3+}$ (A), TIL $_{galectin\text{-}9+}$ and TIL $_{galectin\text{-}9+}$ (B), TIL $_{PD\text{-}1+}$ and TIL $_{PD\text{-}1+}$ (C), TIL $_{PD\text{-}L1+}$ and TIL $_{PD\text{-}L1+}$ (D), TIL $_{OX40+}$ and TIL $_{OX40+}$ (E), TIL $_{OX40L+}$ and TIL $_{OX40L+}$ (F), TIL $_{LAG3+}$ and TIL $_{LAG3+}$ (G), TC $_{MHC\text{-}II+}$ and TIL $_{MHC\text{-}II+}$ (H), TC$^{-}_{KIR2D+}$ and TIL$^{-}_{KIR2D+}$ (I), TC$_{KIR3D+}$ and TIL$_{KIR3D+}$ (J). (K) The column chart of mean distances of positive TILs; P<0.001. (K) The density curves of the distance of TCs and TILs. **Figures S3A* to *3J* were drawn by the "ggplot" package of R software. TC, tumor cell; TIL, tumor-infiltrating lymphocyte; KIR2D, killer cell immunoglobulin-like receptor-2D; KIR-3D, killer cell immunoglobulin-like receptor-3D; TIM-3, T cell immunoglobulin-3; LAG-3, lymphocyte activation gene-3; PD-1, programmed cell death receptor-1; PD-L1, programmed cell death ligand-1; MHC-II, major histocompatibility complex class II; OX40L, OX40-ligand.

http://dx.doi.org/10.21037/tlcr-21-96

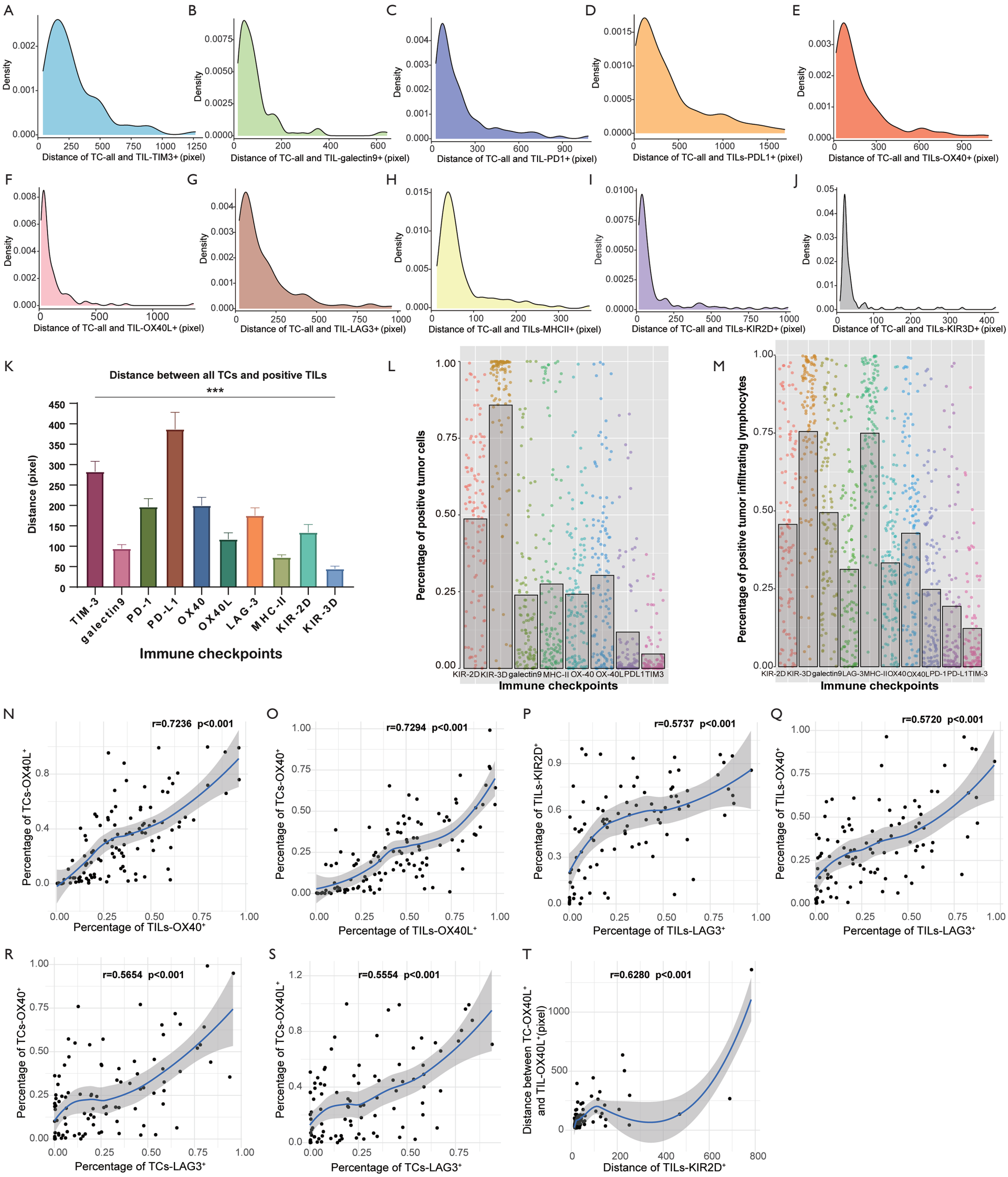

Figure S5 The distribution and correlation of quantitative and spatial data. Density curves of the distance of TC_{all}-TIL_{TIM3+} (A), TC_{all}-$TIL_{galectin-9+}$ (B), TC_{all}-TIL_{PD-1+} (C), TC_{all}-TIL_{PD-L1+} (D), TC_{all}-TIL_{OX40+} (E), TC_{all}-TIL_{OX40L+} (F), TC_{all}-TIL_{LAG-3+} (G), TC_{all}-$TIL_{MHC-II+}$ (H), TC_{all}-TIL_{KIR2D+} (I), TC_{all}-TIL_{KIR3D+} (J). (K) The column chart of mean distances of all TCs and positive TILs, and the error bars showed the standard error of the mean (SEM).; P<0.001. The distribution jitter blot and mean values column chart of the percentage of positive TCs (L) and positive TILs (M). Correlation curves of the percentage of TIL $_{OX40+}$ and the percentage of TC $_{OX40L+}$ (N), the percentage of TIL_{OX40L+} and the percentage of TC_{OX40+} (O), the percentage of TIL_{LAG3+} and the percentage of TIL $_{KIR2D+}$ (P), the percentage of TIL_{LAG3+} and the percentage of TIL_{OX40+} (Q), the percentage of TC_{LAG3+} and the percentage of TC_{OX40+} (R), the percentage of TC_{LAG3+} and the percentage of TC_{OX40L+} (S), the distance of $TILs_{-KIR2D+}$ and the distance between TC_{OX40L+} and TIL_{OX40L+} (T). TC, tumor cell; TIL, tumor-infiltrating lymphocyte; KIR2D, killer cell immunoglobulin-like receptor-2D; KIR-3D, killer cell immunoglobulin-like receptor-3D; TIM-3, T cell immunoglobulin-3; LAG-3, lymphocyte activation gene-3; PD-1, programmed cell death receptor-1; PD-L1, programmed cell death ligand-1; MHC-II, major histocompatibility complex class II; OX40L, OX40-ligand.

http://dx.doi.org/10.21037/tlcr-21-96

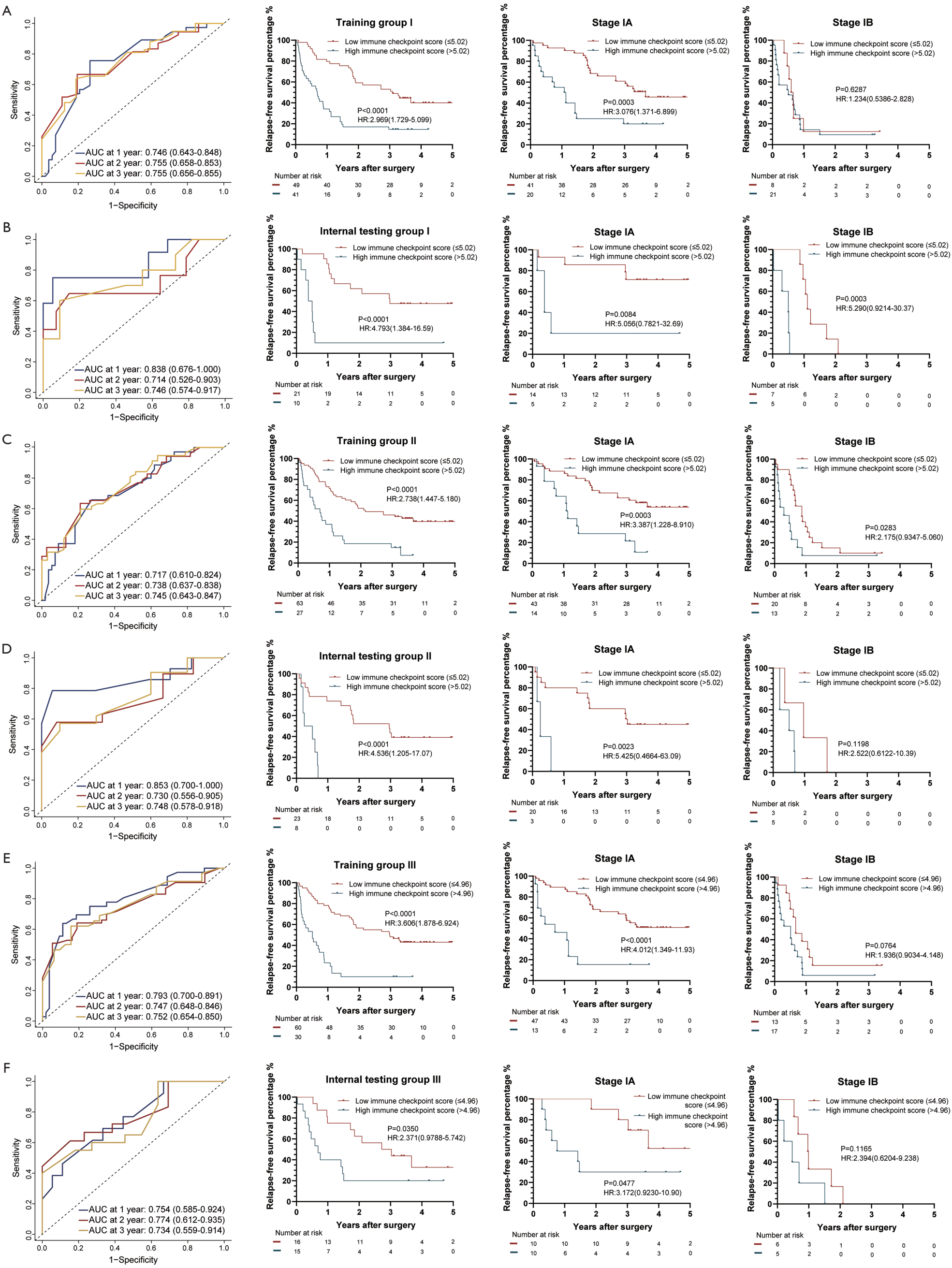

Figure S6 The IC-Score for RFS measured by time-dependent ROC curves and Kaplan–Meier survival in the representative 3 training and testing groups. (A) Training group I; (B) Internal testing group I; (C) Training group II; (D) Internal testing group II; (E) Training group III; (F) Internal testing group III. We used AUCs at 1, 2, and 3 years to assess prognostic accuracy of RFS, and calculated P values using the log-rank test. Data represent AUC or P value. HR, hazard ratio; AUC, area under ROC; ROC, receiver operator characteristic. *The cut-off point was determined by the X-Tile software, and the time-dependent AUC with 95% CI was calculated by the "timeROC" package of R software.

http://dx.doi.org/10.21037/tlcr-21-96

Table S3 The structure of the ResNet used in this study

Layer name	Output size	ResNet-18	ResNet-101	ResNet-152
conv1	112×112	7×7, 64, stride 2		
conv2_x	56×56	3×3 max pool, stride 2		
		$\begin{bmatrix} 3\times3 & 64 \\ 3\times3 & 64 \end{bmatrix}\times2$	$\begin{bmatrix} 1\times1 & 64 \\ 3\times3 & 64 \\ 1\times1 & 256 \end{bmatrix}\times3$	$\begin{bmatrix} 1\times1 & 64 \\ 3\times3 & 64 \\ 1\times1 & 256 \end{bmatrix}\times3$
conv3_x	28×28	$\begin{bmatrix} 3\times3 & 128 \\ 3\times3 & 128 \end{bmatrix}\times2$	$\begin{bmatrix} 1\times1 & 128 \\ 3\times3 & 128 \\ 1\times1 & 512 \end{bmatrix}\times4$	$\begin{bmatrix} 1\times1 & 128 \\ 3\times3 & 128 \\ 1\times1 & 512 \end{bmatrix}\times8$
conv4_x	14×14	$\begin{bmatrix} 3\times3 & 256 \\ 3\times3 & 256 \end{bmatrix}\times2$	$\begin{bmatrix} 1\times1 & 256 \\ 3\times3 & 256 \\ 1\times1 & 1024 \end{bmatrix}\times23$	$\begin{bmatrix} 1\times1 & 256 \\ 3\times3 & 256 \\ 1\times1 & 1024 \end{bmatrix}\times36$
conv5_x	7×7	$\begin{bmatrix} 3\times3 & 512 \\ 3\times3 & 512 \end{bmatrix}\times2$	$\begin{bmatrix} 1\times1 & 512 \\ 3\times3 & 512 \\ 1\times1 & 2048 \end{bmatrix}\times3$	$\begin{bmatrix} 1\times1 & 512 \\ 3\times3 & 512 \\ 1\times1 & 2048 \end{bmatrix}\times3$
	1×1	Average pool, 1000-d fc, softmax		

http://dx.doi.org/10.21037/tlcr-21-96

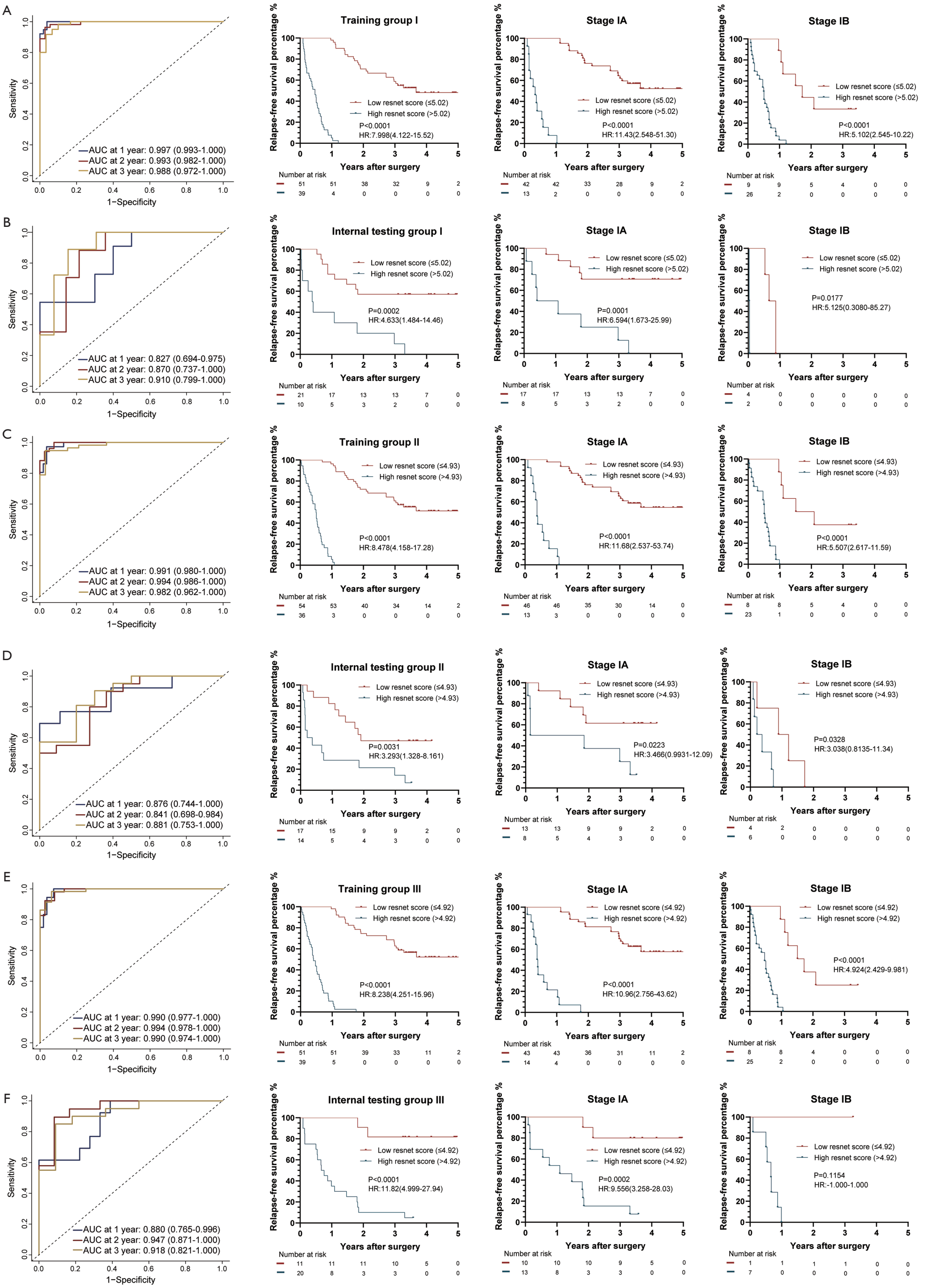

Figure S7 The Res-Score for RFS measured by time-dependent ROC curves and Kaplan–Meier survival in the representative 3 training and testing groups. (A) Training group I; (B) Internal testing group I; (C) Training group II; (D) Internal testing group II; (E) Training group III; (F) Internal testing group III. We used AUCs at 1, 2, and 3 years to assess prognostic accuracy of RFS, and calculated P values using the log-rank test. Data represent AUC or P value. HR, hazard ratio; AUC, area under ROC; ROC, receiver operator characteristic. *The cut-off point was determined by the X-Tile software, and the time-dependent AUC with 95% CI was calculated by the "timeROC" package of R software.

http://dx.doi.org/10.21037/tlcr-21-96

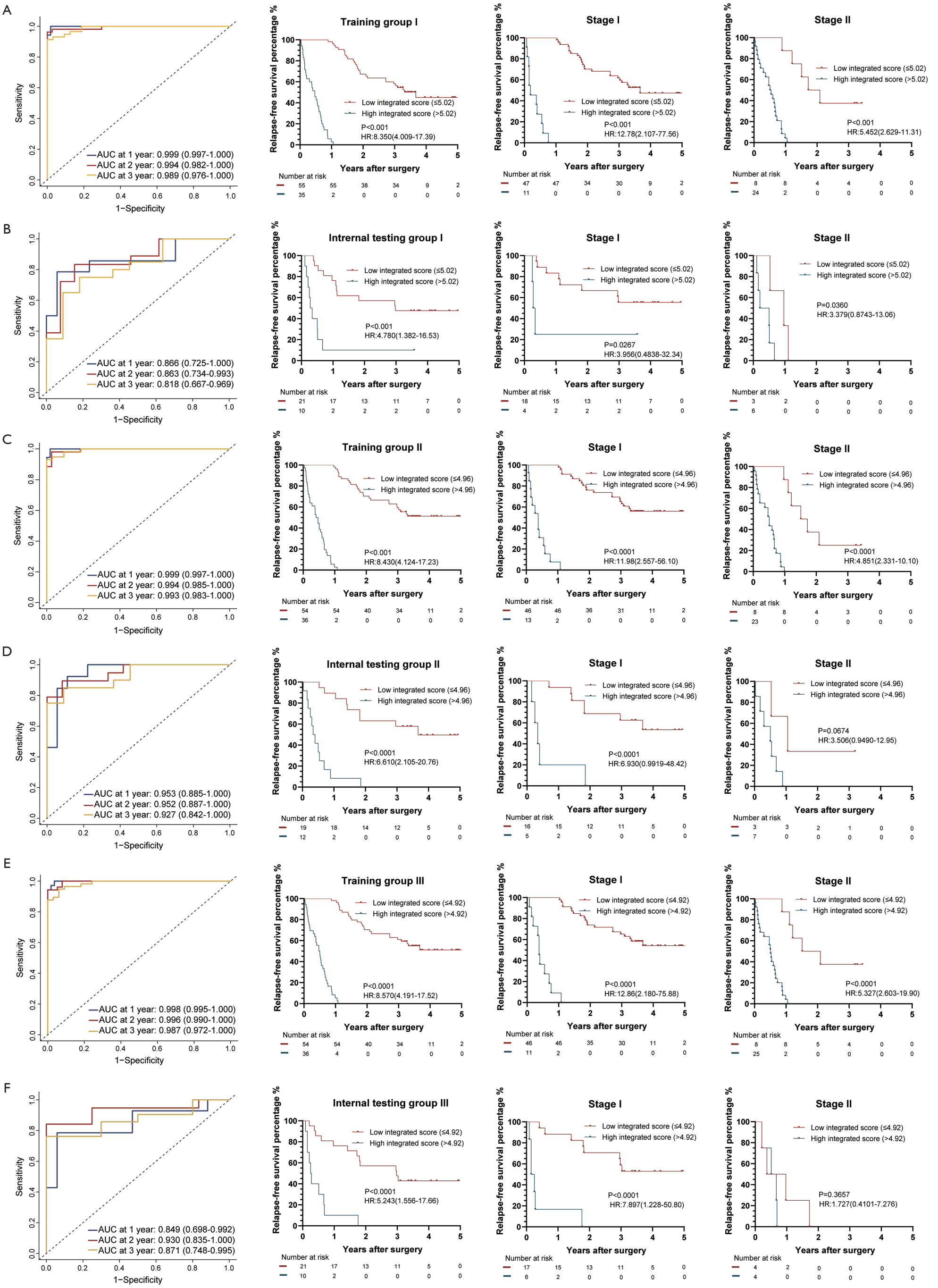

Figure S8 The integrated score for RFS measured by time-dependent ROC curves and Kaplan–Meier survival in the representative 3 training and testing groups. (A) Training group I; (B) Internal testing group I; (C) Training group II; (D) Internal testing group II; (E) Training group III; (F) Internal testing group III. We used AUCs at 1, 2, and 3 years to assess prognostic accuracy of RFS, and calculated P values using the log-rank test. Data represent AUC or P value. HR, hazard ratio; AUC, area under ROC; ROC, receiver operator characteristic. *The cut-off point was determined by the X-Tile software, and the time-dependent AUC with 95% CI was calculated by the "timeROC" package of R software.

http://dx.doi.org/10.21037/tlcr-21-96

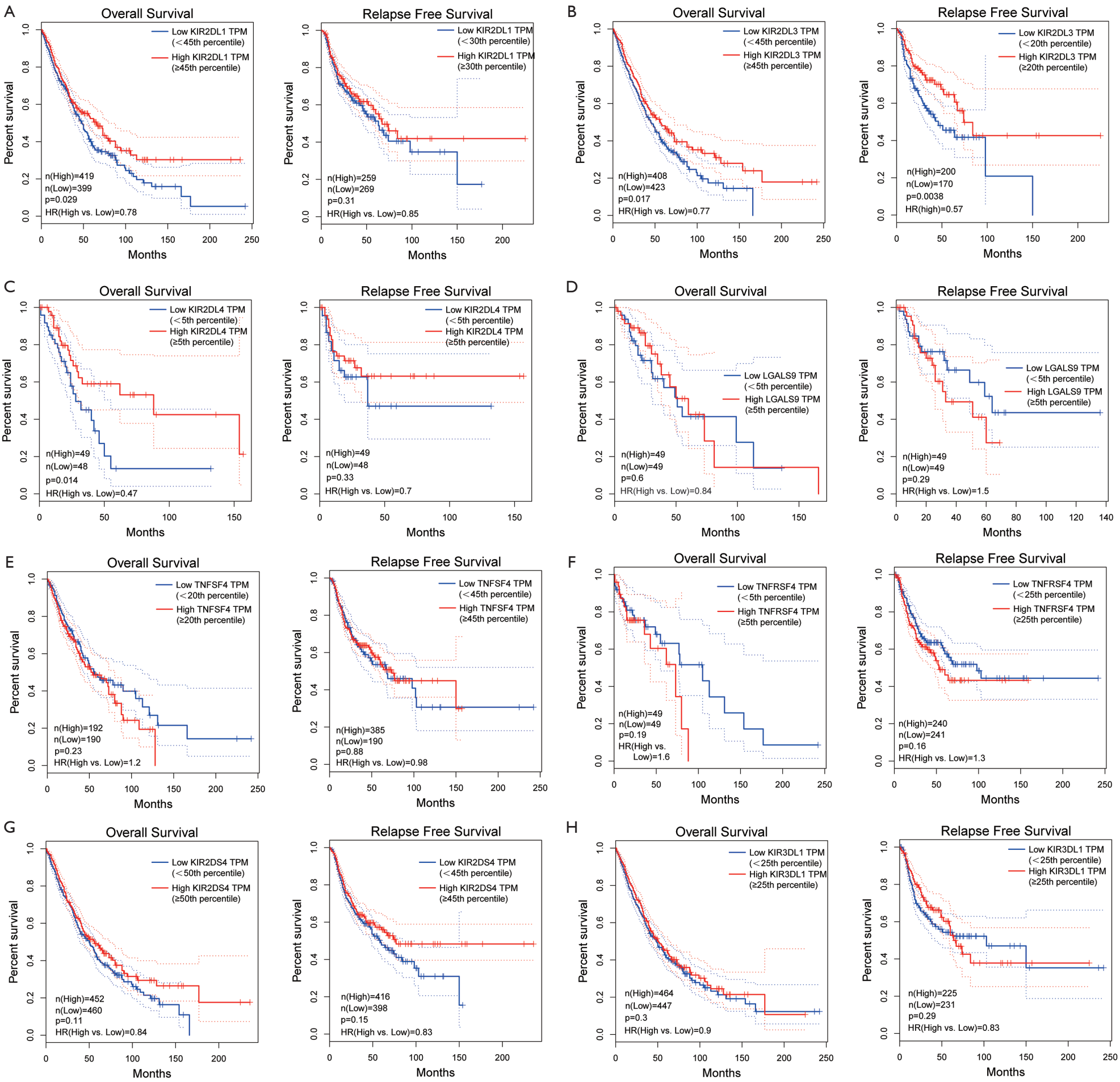

Figure S9 The Kaplan-Meier curves of the gene levels of prognostic immune checkpoints in LUAC and LUSD from the GEPIA dataset. (A) The Kaplan-Meier curves of KIR2DL1 for OS (left) and RFS (right). (B) The Kaplan-Meier curves of KIR2DL3for OS (left) and RFS (right). (F) The Kaplan-Meier curves of KIR2DL4for OS (left) and RFS (right). (C) The Kaplan-Meier curves of KIR2DL3 for OS (left) and RFS (right). (D) The Kaplan-Meier curves of LGALS9 (galectin-9) for OS (left) and RFS (right). (E) The Kaplan-Meier curves of TNFSF4 (OX40) for OS (left) and RFS (right). (F) The Kaplan-Meier curves of TNFRSF4 (OX40L) for OS (left) and RFS (right). (G) The Kaplan-Meier curves of KIR2DS4 for OS (left) and RFS (right). (G) The Kaplan-Meier curves of KIR3DL1 for OS (left) and RFS (right). LUAC, lung adenocarcinoma; LUSC, lung squamous cell carcinoma; HR, hazard ratio; OS, overall survival; RFS, relapse-free survival; KIR2D, killer cell immunoglobulin-like receptor-2D; KIR-3D, killer cell immunoglobulin-like receptor-3D; TPM, transcripts per kilobase million.

http://dx.doi.org/10.21037/tlcr-21-96

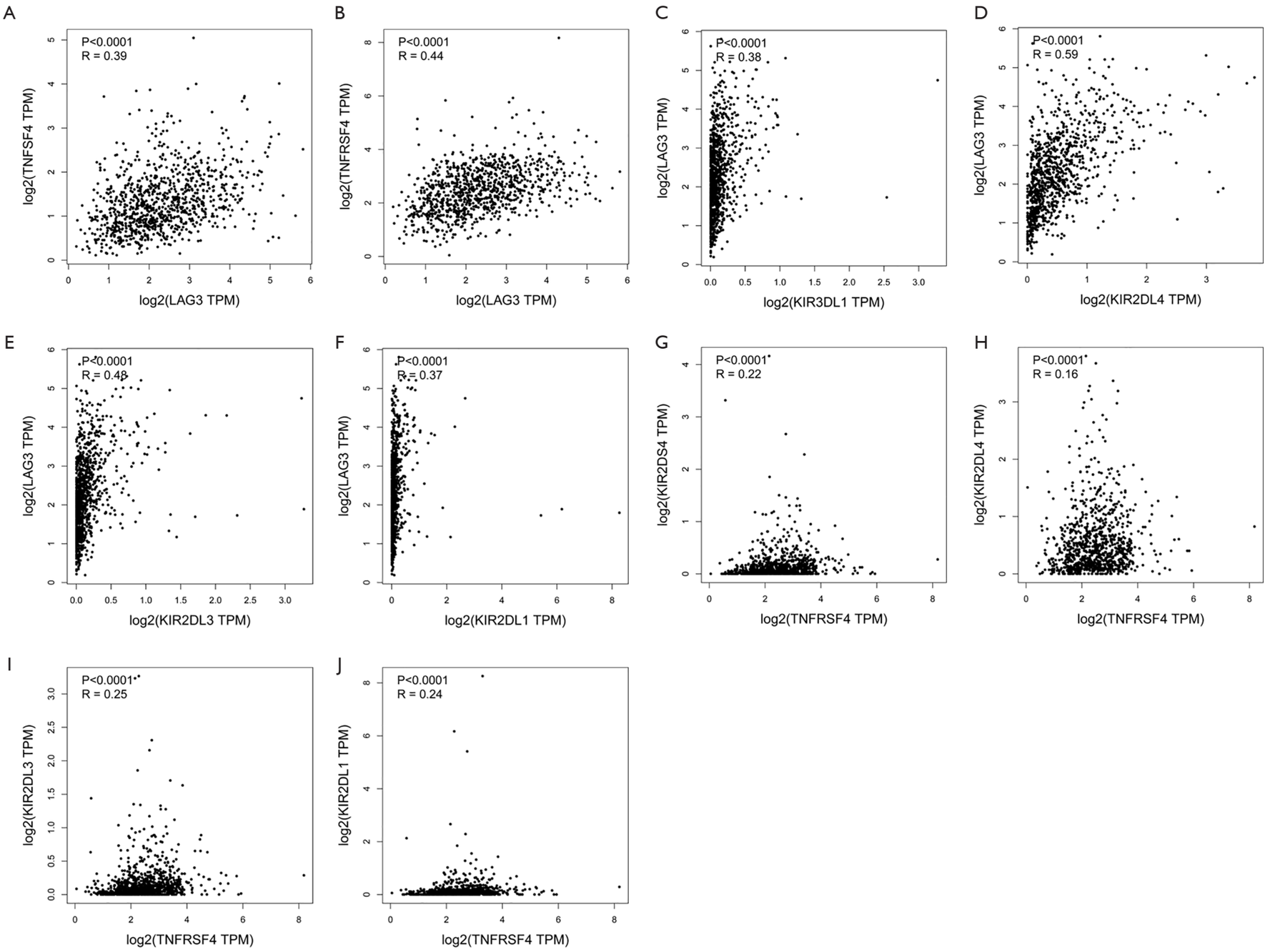

Figure S10 The correlation analysis for gene levels of immune checkpoints proteins in LUAC and LUSD from the GEPIA dataset. The Spearman correlation analysis of (A) LAG3-TNFSF4 (OX40), (B) LAG3-TNFRSF4(OX40L), (C) LAG3-KIR3DL1, (D) LAG3-KIR2DL4, (E) LAG3-KIR2DL3, (F) LAG3-KIR2DL1, (G) TNFRSF4(OX40L)-KIR2DS4, (H) TNFRSF4(OX40L)-KIR2DL4, (I) TNFRSF4(OX40L)-KIR2DL3, (J) TNFRSF4(OX40L)-KIR2DL1. LUAC, lung adenocarcinoma; LUSC, lung squamous cell carcinoma; KIR2D, killer cell immunoglobulin-like receptor-2D; KIR-3D, killer cell immunoglobulin-like receptor-3D; LAG-3, lymphocyte activation gene-3; TPM, transcripts per kilobase million.

http://dx.doi.org/10.21037/tlcr-21-96

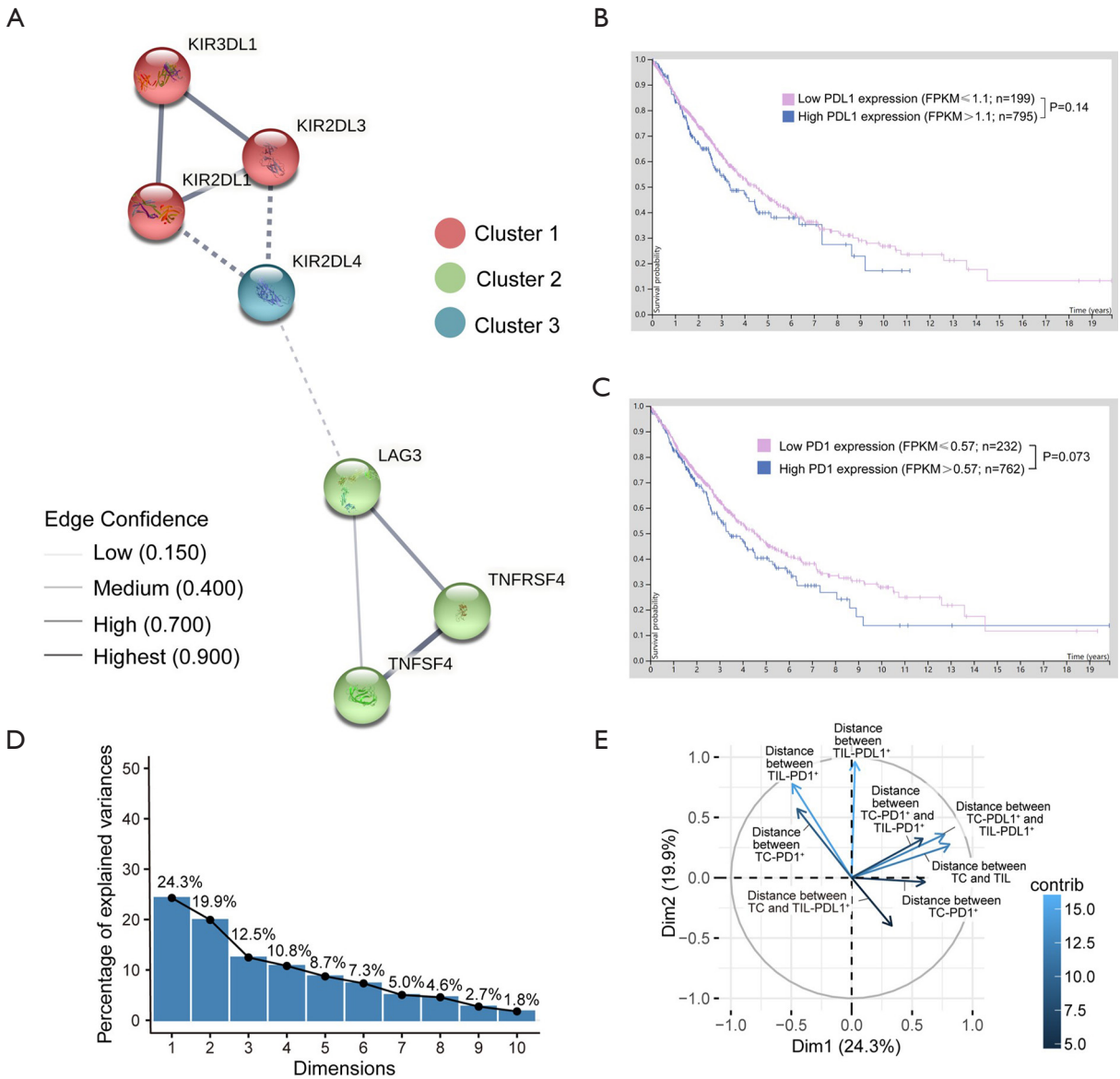

Figure S11 (A) The STRING protein-protein interaction network. Network of the interactions among LAG3, TNFSF4 (OX40), TNFRSF4 (OX40L), KIR2DL1, KIR2DL3, KIR2DL4, and KIR3DL1. The line thickness between two proteins indicates the strength of data support, and the edges indicate both functional and physical protein associations. Different colors represent the cluster via the k-mean clustering. (B) The Kaplan-Meier curves of the mRNA level of PD-L1 for overall survival in LUAC and LUSC from the HPA database. (C) The Kaplan-Meier curves of the mRNA level of PD-1 for OS in LUAC and LUSC from the HPA database. (D) The bar chart on the percentage of explained variance of each dimension from the PCA. (E) The contribution (contrib) and the quality of the representation(cos2) od each feature in dimension 1 (Dim.1) and dimension (Dim.2). The deeper of the color, the more contribution was made by the feature. The closer a variable is to the circle of correlations, the better its representation on the factor map. STRING, Search Tool for the Retrieval of Interacting Genes/Proteins; LUAC, lung adenocarcinoma; LUSC, lung squamous cell carcinoma; KIR2D, killer cell immunoglobulin-like receptor-2D; KIR-3D, killer cell immunoglobulin-like receptor-3D; LAG-3, lymphocyte activation gene-3; PD-1, programmed cell death protein; PD-L1, programmed death-ligand 1; TC, tumor cell; TIL, tumor infiltrating lymphocytes; FPKM, fragments per kilobase of exon model per million mapped fragments; HPA, human protein atlas.

http://dx.doi.org/10.21037/tlcr-21-96

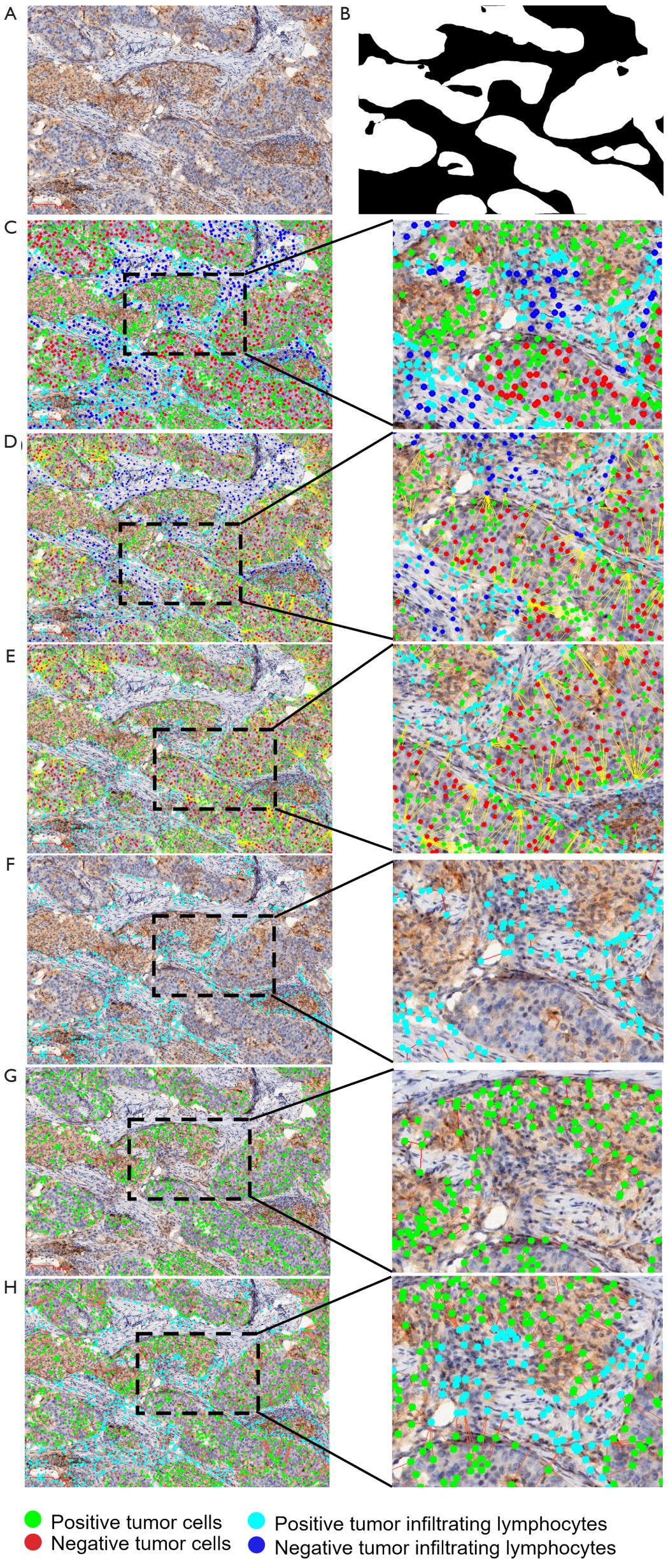

Figure S12 The representative images of segmentation and spatial analysis of the in external cohort. The original IHC image (A), tumor region segmentation mask (B), four classifications of cells(C), the distance of all TCs and all TILs (D), the distance of all TCs and TIL-PDL1$^+$ (E), the distance of TIL-PDL1$^+$ (F), the distance of TC-PDL1$^+$ (G), the distance of TC-PDL1$^+$ and TIL-PDL1$^+$ (H). Green dots represented positive TCs; red dots represented negative TCs; light blue represented positive TILs; dark blue represented negative TILs; and the red or yellow lines between cells were straight line distance between two cells. IHC, immunohistochemistry; PDL1, programmed death-ligand 1; TC, tumor cell; TIL, tumor-infiltrating lymphocyte.

http://dx.doi.org/10.21037/tlcr-21-96